Progress in Organic Coatings 222 (2027) 110630

Contents lists available at ScienceDirect

Progress in Organic Coatings

journal homepage: www.elsevier.com/locate/porgcoat

Biobased binder formulation for screen printing cellulosic textiles with sea buckthorn-derived natural dyes

Ritesh Sharma [a], Mikko Herrala [b], Jenni Tienaho [c], Riikka Haapala [b], Jaana Rysä [b], Ali Tehrani-Bagha [a], Paula Nousiainen [a,*]

[a] Department of Bioproducts and Biosystems, Aalto University, Vuorimiehentie 1, 02150, Espoo, Finland
[b] School of Pharmacy, University of Eastern Finland, Yliopistonrinne 3, 70210, Kuopio, Finland
[c] Production Systems, Natural Resources Institute Finland (Luke), Latokartanonkaari 9, 00790, Helsinki, Finland

ARTICLE INFO

Keywords:
Biobased binder
Natural dye printing
Agricultural waste valorization
Skin-compatibility
Antimicrobial textiles

ABSTRACT

The growing demand for sustainable textile manufacturing has intensified the search for renewable alternatives to petroleum-based dyes and binders used in textile printing. However, the industrial adoption of natural dyes remains limited by poor dye fixation, inadequate durability, and the lack of bio-based binder systems capable of delivering high printing performance. In this study, a bio-based, water-borne printing paste was developed by combining a chitosan–cationic starch binder with a natural dye extracted from sea buckthorn pomace, an agricultural by-product, for screen printing of cellulosic textiles. The formulation was optimized using zeta potential, quartz crystal microbalance with dissipation (QCM-D), and rheological analyses to understand dye–-binder interactions and establish suitable printing conditions. At 3% dye concentration, the biobased paste produced uniform prints with approximately twice the color strength of the commercial polyurethane-based binder (K/S = 3.07 vs. 1.53). The printed textiles also demonstrated good wash, rub, and perspiration fastness, with tactile comfort comparable to that of the commercial system. In addition, the bio-based formulation exhibited antimicrobial activity against *Escherichia coli* and *Staphylococcus aureus*, which was retained in the printed textiles after washing. The sea buckthorn dye showed no skin-sensitizing potential under the tested conditions, while cytotoxicity and oxidative stress were observed only at high concentrations. Overall, this study demonstrates that agricultural waste-derived natural dyes, combined with a biobased binder, can produce durable, multifunctional, and skin-compatible printed textiles, offering a promising platform for biobased textile printing systems with natural dyes.

1. Introduction

The textile industry is one of the most resource-intensive and environmentally impactful sectors, primarily due to its dependence on fossil-based chemicals, high water consumption, and the generation of hazardous effluents. Textile dyeing and printing processes significantly contribute to this issue, responsible for approximately 17–20% of industrial water pollution due to the discharge of dyes and auxiliaries containing wastewater [1]. A large fraction of the dyes remains unfixed during processing and is released into the aquatic environment without proper treatment, where they persist due to their complex structures and pose risks to both ecosystems and human health [2]. In addition, the conventional textile printing industry relies extensively on petroleum-derived polymeric binders, creating an additional dependence on fossil resources. Many synthetic dyes are also reported to be toxic, carcinogenic, and resistant to degradation, which leads to environmental contamination [3]. These challenges have driven increasing interest toward biobased dyes and fully biobased binder systems for textile printing applications that can reduce fossil-resource dependence while maintaining performance required for the textile printing process.

Textile printing is an important and unique method for introducing color and design to textile materials. From a methodological standpoint, textile printing is one of the most accessible and versatile techniques to bring design ideas, diverse shades of color, and a textile substrate together. A variety of printing systems, including pigment, reactive, and disperse printing, are utilized depending on the fiber composition and end-use applications [4,5]. Among these, pigment-based printing is widely used due to its compatibility with different fiber types and

* Corresponding author.
E-mail address: paula.nousiainen@aalto.fi (P. Nousiainen).

https://doi.org/10.1016/j.porgcoat.2026.110630
Received 10 July 2026; Received in revised form 4 September 2026; Accepted 13 September 2026

relatively simple processing conditions.

A typical formulation in textile printing consists of dyes, binders, thickeners as a rheology modifier, antifoaming agents, and softeners. Almost all these materials originate from fossil-based sources. In pigment printing, the dye itself lacks inherent affinity for the textile substrate, particularly toward cellulosic fibers like cotton [6]. Therefore, a film-forming binder is essential to attach pigments or dye particles to the fabric surface during the drying and curing process [7]. While synthetic binders provide excellent durability and colorfastness properties, they are often non-biodegradable, non-renewable, and potentially toxic [8]. During textile printing and subsequent washing, unfixed binder components and other printing auxiliaries can enter the wastewater, increasing its chemical and organic load and potentially leaving persistent polymeric residues. Furthermore, the conventional textile printing methods generate large volumes of wastewater and release harmful chemicals like formaldehyde, urea, and melamine into the environment [9,10], further increasing wastewater treatment burden. The extensive use of fossil-based binders, particularly acrylics and polyurethane, contributes to the overall environmental footprint of the textile printing process [11].

The revival of natural dyes and colorants extracted from various plant sources, non-food materials, and insects has gained attention in the textile industry owing to their biodegradability, lower toxicity, and alignment with sustainable development goals [12]. Despite their ecological advantages, the widespread adoption of natural dyes has remained limited due to the lack of standardized shade cards and application protocols [13]. Additionally, the low substantivity of natural dyes toward textile substrates is a key challenge, particularly in pigment printing, where the dye is deposited on the surface rather than penetrating the fibers [14]. In surface-based printing applications, insufficient dye–substrate interactions can result in poor wash fastness and light fastness. Binders therefore play an important role by anchoring the colorant to the fiber surface and forming a continuous film that improves durability [15]. Despite increasing interest in natural colorants, fully biobased binder systems specifically suited to natural-dye textile printing remain limited, and petroleum-derived binders are still commonly used to achieve adequate fixation and colorfastness.

In parallel, low-water or waterless coloration technologies have been increasingly explored to reduce water consumption and wastewater generation in textile wet-end processing. Advanced technologies such as digital printing, low-liquor processing, and non-aqueous systems using supercritical carbon dioxide or polalkylsiloxanes can substantially decrease or, in some cases, even eliminate the need for water during coloration [16–18]. However, these processes primarily address water and process efficiency and do not necessarily resolve the material-related challenges associated with the composition of printing formulation. Therefore, the development of renewable binder systems compatible with natural dyes represents a complementary material-level strategy toward the natural dye textile printing process.

Recent studies have explored various biobased-binder systems for natural dye printing, which often involve multifunctional additives, chemical crosslinkers, mordanting strategies, or complex formulations to enhance dye-substrate interactions. These systems, while effective, consist of multi-step preparation protocols [8], additional crosslinkers [9], or mordants [19], complicating scalability and reproducibility. Therefore, naturally derived polymers such as chitosan- and starch-based derivatives can provide an eco-friendly option due to their biodegradability, biocompatibility, and low toxicity, along with their widespread use in various sectors such as textile, biomedical, and food-related applications.

To address the gap in natural-dye textile printing, we introduced a water-borne biobased binder formulation free of fossil-based auxiliaries, designed to improve compatibility with natural dyes while enhancing durability and user safety. Unlike conventional approaches that rely on metal mordants or petroleum-derived binders for adequate dye fixation and durability, our formulation provides a biobased alternative. The formulation was systematically optimized by utilizing surface-sensitive techniques such as zeta potential and Quartz Crystal Microbalance with dissipation (QCM-D), and rheological profiling to elucidate dye-binder interactions and define suitable printing conditions. The performance of the printed textiles was evaluated via colorfastness testing and sensorial assessment using the Fabric Touch Tester (FTT). We also investigated the antimicrobial activity of the biobased binder, dye, and printed substrates and, considering the growing emphasis on skin-friendly materials, assessed the skin-sensitization of the sea buckthorn-derived dye. Altogether, this work demonstrates a comprehensive strategy for developing an eco-friendly, multifunctional biobased binder system tailored to natural-dye textile printing.

2. Experimental

2.1. Materials

The fabric used in printing was a bleached knitted cotton (single jersey, 24 Ne course and wale, 150 g/m^2) obtained from Orneule Knitting Company (Tampere, Finland). The reference sample exhibited a whiteness value of 77.09, with corresponding CIELAB color coordinates of L* = 93.91, a* = −40, and b* = 1.73.

Sea buckthorn berry pomace remaining after juice extraction was obtained from a local producer in southern Finland. Polyamide (PA) filters with a 200 μm mesh opening were from Sefar Nitex (Switzerland), and filter paper with a pore size of 12–15 μm was from VWR (Finland). The printing screen was obtained from A. Wennström Ltd. (Artjärvi, Finland). The non-ionic detergent for soaping and washing fastness procedures was from SDC-Germany. Cellulose nanofibrils (CNF) used for cellulose model surfaces in QCM-D studies were prepared from a 1.95 wt % fluidized never-dried hardwood birch pulp suspension. QCM-D gold crystals were from Biolin Scientific (Sweden). Polyethylenimine (PEI, Mw 50,000–100,000), used as an anchoring agent for CNF deposition, was obtained from Sigma-Aldrich. The high molecular weight chitosan (HMW Cht, Mw 310,000–375,000, >75% deacetylated) was purchased from Sigma-Aldrich (Merck, Darmstadt, Germany), and Cationic Starch was from Chemigate Oy (Lapua, Finland). A polyurethane (PU) based binder (A-5001, aroma-free and hydrocarbon-rich weighted paste) was obtained from Wennström Oy (Artjärvi, Finland). Ethanol (EtOH, ≥99.9%) for dye extraction was obtained from Anora Group Oy (Finland). Glycerol (1,2,3-propanetriol, ≥99.9%), used as a plasticizer, and acetic acid (glacial, ACS reagent, ≥99.7%), used as a pH adjuster, were from Sigma-Aldrich.

The reagents used for the toxicity assessment of the sea buckthorn extract included 3-[4,5-dimethylthiazol-2-yl]-2,5-diphenyl tetrazolium bromide (MTT), dimethyl sulfoxide (DMSO), menadione, propidium iodide (PI), Triton X-100, and fetal bovine serum (FBS), all obtained from Sigma-Aldrich (USA/Germany). The CyQUANT lactate dehydrogenase (LDH) cytotoxicity assay kit and MitoSOX Red reagent were from Invitrogen (USA/UK). Digitonin was from Calbiochem (Germany), and dihydroethidium (DHE) from Fluka BioChemica (Switzerland). Cell culture reagents, including Dulbecco's Modified Eagle Medium (DMEM), Dulbecco's Phosphate Buffered Saline (DPBS), L-glutamine, and trypsin-ethylenediaminetetraacetic acid (EDTA), were from Gibco (UK). Hanks' Balanced Salt Solution (HBSS) was from Euroclone (Italy). Erythrosin B stain was from Logosbio (South Korea). The in vitro skin sensitization testing was conducted using the instaCELL™ KeratinoSens™ assay kit from acCELLerate (Germany). Penicillin/streptomycin was from Lonza (Switzerland). All reagents were used as received without further purification.

The chemicals used in the antibacterial assessment, including Tryptone (peptone from casein), yeast extract (bacteriological), and sodium chloride (AnalaR), were from VWR Chemicals. Ampicillin sodium salt (BioScience Grade) was from Carl Roth, and erythromycin (BioReagent, suitable for cell culture) was from Sigma-Aldrich.

2.2. Methods

2.2.1. Dye extraction

The dye was extracted from 300 g of Sea Buckthorn berries pomace using a 1:3 material-to-liquor ratio with a solvent mixture of 75% ethanol and 25% deionized water. The mixture was blended to a homogeneous consistency and allowed to stand for 24 h. The liquor was separated using a Sefar Nitex PA filter with a mesh opening of 200 μm, followed by filtration with a 12–15 μm pore size filter paper. The filtrate was centrifuged at 9900 rpm for 30 min, and the supernatant was collected. The supernatant was freeze-dried using a Labconco FreeZone 2.5 L system at −40 °C and 0.250 mBar for 24 h, yielding approximately 24 g of dry extract (8% yield, based on the initial dry mass of sea buckthorn pomace).

2.2.2. Preparation of chitosan and cationic starch solutions for binder formulation

To formulate the fully biobased binder, an initial formulation optimization was carried out using various weight-to-volume (*w/v*) concentrations of chitosan and cationic starch (Table S1). Through a systematic evaluation of rheology and printing performance supported by previously reported biobased binder formulation [20,21], the combination of 2% chitosan (*w/v*) and 4% cationic starch (*w/v*) was found optimal.

For solution preparation, 2 g of high-molecular-weight chitosan (HMW Cht) was dissolved in 100 mL of distilled water at 60 °C with the dropwise addition of 1% (*v*/v) acetic acid (1 mL) under continuous stirring using a Heidolph RZR 2051 mechanical overhead stirrer. The solution was stirred continuously for 4 h at 500 rpm until a clear and homogeneous solution was obtained.

Similarly, the cationic starch solution was prepared by dissolving 4 g of cationic starch in 100 mL of distilled (DI) water. First, DI water was heated to 95 °C, and then the cationic starch was gradually added while stirring constantly at 500 rpm using a Heidolph RZR 2051 overhead stirrer until homogeneous.

2.2.3. Preparation of printing pastes and textile screen printing process

To formulate a fully biobased printing paste, a previously dissolved chitosan solution (2% *w/v*) was added gradually with pregelatinized cationic starch solution (4% *w/v*) at a 1:1 ratio and stirred for 30 min to promote homogeneous mixing and electrostatic interaction between the two polysaccharides. Glycerol (5% *w*/w), acting as a plasticizer, was added to the formulation to enhance the flexibility and film-forming ability of the binder and stirred for 30 min to ensure uniform dispersion. Finally, the required concentration of natural dye (1, 3, and 5% *w*/w) was added, and the entire formulation was stirred for an additional 1 h to obtain a uniform, viscous printing paste (Table 1).

Prior to printing trials, the final formulation was allowed to equilibrate for 30 min to ensure rheological stability.

Textile printing on cotton fabric was carried out using a manual flatbed screen printing technique. A screen-printing mesh T43, characterized by 43 threads/cm and a yarn thickness of 64 μm, was employed. Printing was carried out under ambient conditions, using a rubber squeegee with an angle to maintain uniform paste application across all samples.

The printed samples were dried in an oven at 80 °C for 30 min, followed by curing in a hydraulic hot press (Vakomet KRO-260, Lakeuden Hydro Oy, Finland) at 160 °C for 2 min under 100 kN pressure to promote color fixation. To remove any unfixed dyes, the printed samples were washed with a non-ionic detergent (2 g/L) at a liquid-to-fabric ratio of 1:20 at 40 °C for 30 min.

Table 1
Formulation of a biobased (BB) and synthetic (SB) binder system.

Sample code[a]	Chitosan 2% *w/v* (g)	Cationic starch 4% w/v (g)	Synthetic binder (g)	Dye (g)	Glycerol (g)	Total (g)
$BB_{1\%}$	23.5	23.5	–	0.50	2.50	50
$BB_{3\%}$	23	23	–	1.50	2.50	50
$BB_{5\%}$	22.5	22.5	–	2.50	2.50	50
$SB_{1\%}$	–	–	49.50	0.50	–	50
$SB_{3\%}$	–	–	48.50	1.50	–	50
$SB_{5\%}$	–	–	47.50	2.50	–	50

[a] BB = Biobased binder, SB = Synthetic binder; 1%, 3%, and 5% refer to the dye concentration used.

2.3. Characterization

2.3.1. Zeta potential measurement

To find an optimal pH for the printing paste, the electrophoretic mobility of sea buckthorn extract, chitosan, cationic starch, and biobased binder in different pH buffer solutions was measured with a Zetasizer Nano ZS 90 Solutions (Malvern Instruments, UK). The zeta potential was obtained from electrophoretic mobility data using the Smoluchowski model. All the measurements were performed in triplicate, and the results are reported as mean values with corresponding standard deviations.

2.3.2. Quartz crystal measurements with dissipation (QCM-D)

To investigate the adsorption kinetics of dye, chitosan, and cationic starch on cellulosic substrates, QCM-D measurements were carried out using a Q-Sense E4 instrument (Q-Sense, Sweden). In these experiments, cellulose nanofiber (CNF) thin films were used as a model substrate to represent cellulosic fibers. The CNF thin films were prepared via a spin-coating process on 14 mm diameter QCM-D quartz crystal resonators with gold electrodes (Biolin Scientific, Sweden). PEI with a concentration of 2.5 mg/mL was used as an anchoring layer to facilitate a strong attachment of CNF fibrils to the crystal surface. A CNF suspension (0.1 wt%), containing primarily the finest fibrils, was spin-coated onto resonators at 4000 rpm for 1 min.

The adsorption studies were carried out at pH 5, selected based on the zeta potential optimization. Initially, the CNF-coated crystals were equilibrated with a 1% acetic acid buffer (pH 5) until a stable baseline was achieved. Subsequently, chitosan and cationic starch (0.1 g/L, pH 5) were sequentially introduced into the chamber, and frequency and dissipation shifts (3rd overtone) were monitored. Once a plateau in frequency was reached, indicating complete adsorption of chitosan and cationic starch onto CNF films, the excess solution was rinsed using the same pH 5 buffer. Next, a dye solution (0.1 g/L) at pH 5 was introduced into the chamber under similar conditions to monitor their adsorption kinetics for 90 min. A final rinse step was performed to remove any loosely bound dye.

The adsorbed mass on the CNF film surface was calculated using the Sauerbrey equation [22]

$$\Delta m = -C.\frac{\Delta f}{n} \quad (1)$$

where Δm represents the adsorbed mass change per unit area (ng/cm^2), C is the sensitivity constant of the quartz crystals (17.7 ng/cm^2 for gold crystals), Δf denotes the measured frequency shift (Hz) during the adsorption process, and n is the overtone number corresponding to the oscillation frequency.

2.3.3. Rheological properties of binder and printing paste

The rheological behavior of the formulated biobased binder, corresponding bioprinting paste, commercial synthetic binder, and synthetic binder with natural dye was studied to understand their flow and viscoelastic properties, which are critical for printability and film formation. Flow curves ($\eta = f(\dot{\gamma})$) were performed with a setting of σ = 0.1–1000 Pa, covering a wide shear stress range to simulate both low-

shear storage and high-shear application that occurs during textile screen printing. The samples were subjected to a controlled stress mode using a Physica MCR 301 rotational rheometer (Anton Paar GmbH, Austria), equipped with a cone-plate geometry with a 25 mm diameter and a 1° angle. All the measurements were carried out at 25 °C. The equipment was a computer-controlled Rheometer software program with temperature control.

2.3.4. Thermogravimetric analysis (TGA) of binder formulation and printing paste

TGA was carried out using a NETZSCH STA 449 F3 Jupiter (Netzsch, Selb, Germany) simultaneous thermal analyzer. Approximately 5–10 mg of each freeze-dried sample (i.e., biobased binder, PU-based synthetic binder, printing paste (dye-loaded formulation), and dye powder) was individually placed in an alumina crucible (Ø 6.8 mm, 85 µL). Thermogravimetric analysis was performed from 40 to 800 °C at a 10 °C min^{-1} heating rate under a nitrogen atmosphere.

2.3.5. In vitro toxicity testing of sea buckthorn dye

Human hepatic (ATCC HB-8065) HepG2 cells were used to determine the cytotoxicity and reactive oxygen species (ROS) production of sea buckthorn extract. The extract was also tested for skin sensitization potential. The cells were cultured in DMEM (1.0 g/L glucose), supplemented with 10% FBS, 1% L-glutamine, 100 U/mL penicillin, and 100 µg/mL streptomycin. For the experiments, 100,000 cells per well were seeded in 48-well plates 24 h prior to exposure. Cell cultures were maintained in 75 cm^2 cell culture flasks in a humidified incubator, with 5% CO_2 at 37 °C.

Powdered extract (100 mg) was dissolved in 1 mL of DMSO to obtain a 100 mg/mL stock solution. The highest concentration of DMSO was kept below 1%, since DMSO may influence cell viability and proliferation [23]. The extract solution was diluted with DMSO and cell culture medium to reach the final concentrations of 0.03–1 mg/mL. In addition, 1% DMSO was used as a vehicle control, and Triton X-100 or menadione was used as a positive control in toxicity studies.

After 24 h of exposure to the extract, cell viability in HepG2 cells was assessed with the MTT assay. Further, apoptotic and necrotic cytotoxicity was measured using the LDH and propidium iodide assays following the test outline of our previous research [24,25]. Cytoplasmic ROS and mitochondrial superoxide production were quantified after 24 h exposure to the extract using the fluorescent probes DHE and MitoSOX Red, respectively [24,25]. DHE is a probe that reacts with intracellular ROS to form fluorescent oxidation products that can be measured, while MitoSOX Red is a DHE derivative that enters mitochondria and reacts with mitochondrial superoxide to form a fluorescent compound.

2.3.6. Skin sensitization

A preliminary study with the commercial KeratinoSens assay kit was performed to assess the skin sensitization potential of the dye, similar to our previous studies [24–26]. The assay is based on luciferase Nrf2 gene activation in skin keratinocytes, which is considered the second key event in the skin sensitization Adverse Outcome Pathway [27].

In brief, the assay-ready keratinocytes were thawed and seeded onto 96-well plates at 10,000 cells per well and pre-incubated for 24 h in a humidified incubator at 37 °C with 5% CO_2, after which the cells were exposed to the extract for 48 h. In exposure experiments, 12 extract concentrations (from 0.49 to 1000 µg/mL) were used, with three parallel wells per concentration. In addition, 1% DMSO was used as a vehicle control, and ethylene glycol dimethacrylate was used as a positive control. After 48-h exposure, cell viability was defined with resazurin, and reporter gene activation with One-Glo reagent. Induction results were considered positive if gene activation was increased by 50%.

2.3.7. Antibacterial assessment

2.3.7.1. Antibacterial assays using luminescent bacterial strains. The antibacterial activity was assessed using luminescent Gram-negative *E. coli* K12+pcGLS11 and Gram-positive *S. aureus* RN4220+pAT19, both expressing chromosomally integrated *lux* genes that produce continuous bioluminescence. Antibacterial effects were quantified as concentration-dependent reductions in light signal, enabling rapid viability assessment [28]. Detailed methods and bacterial cultivation conditions have been published [29]. In brief, strains were stored at −80 °C in 80% glycerol and cultivated on lysogeny agar with ampicillin and phosphate buffer (*E. coli*) and erythromycin (*S. aureus*) to ensure selection pressure. Overnight pre-cultures were grown under shaking at 300 rpm at 30 °C (*E. coli*) or 37 °C (*S. aureus*).

2.3.7.2. Microplate-based luminescence inhibition assay. Samples (0.25, 0.5, and 1 mg/mL) were tested in triplicate in opaque white 96-well plates with positive (ethanol) and negative (double-distilled water) controls. Equal volumes of bacterial suspension were added, and luminescence was recorded every 5 min for 60 min using a Varioskan LUX Multilabel Reader (ThermoFisher Scientific, Waltham, MA, USA). Antibacterial activity was expressed as % inhibition at 60 min relative to the negative control, after the signal had stabilized [30].

$$Inhibition\ (\%) = \left[1 - \left(\frac{RLU(sample)}{RLU\ (control)}\right)\right] \times 100 \quad (2)$$

where RLU represents Relative light units, corresponding to the bioluminescence signal emitted by the bacterial cells.

2.3.7.3. Soft agar overlay imaging assay. Surface activity was evaluated using a soft agar overlay method [29]. Bacteria were mixed with soft agar and poured over samples on 6-well agar plates. Luminescence was imaged using a SPECTRAL Lago X in vivo imaging system (Spectral Instruments Imaging, AZ, USA) and quantified as photons/s/cm^2/sr. Signals were normalized to control wells and expressed as inhibition percentages [31].

2.4. Evaluation of printing quality

2.4.1. Determination of color depth by CIELab and K/S of printed cotton fabrics

The color properties of the printed samples were evaluated in terms of CIE L*, a*, and b* coordinates together with reflectance values using a Ci7600 Sphere (X-Rite, USA) spectrophotometer equipped with a D65 illuminant, a wavelength range of 360–780 nm, and a 10° standard observer. The color strength value (K/S) was calculated by the Kubelka–Munk Eq. (3)

$$\frac{K}{S} = \frac{(1-R)^2}{2R} \quad (3)$$

where K is the absorption coefficient of the fabric to be tested, S is the scattering coefficient of the fabric to be tested, and R is the reflectance at the maximum absorption wavelength. The wavelength of 420 nm was used for the reflectance values.

2.4.2. Print sharpness

Print sharpness was evaluated using high-resolution digital photographs of the standardized pattern (Aalto University logo) with well-defined fine edges on the fabric substrates. The selected regions of the printed motifs were digitally magnified and visually examined. The magnified images were evaluated for potential paste spreading, edge definition, and line continuity.

2.4.3. Ink penetration

Ink penetration of the samples was calculated by determining the ratio of the K/S value obtained from the back of the printed fabric with respect to the value obtained from the face of the printed fabric [32]. Ink penetration was expressed as the penetration factor (P) and calculated using Eq. (4).

$$P\,(\%) = \frac{100\left(\frac{K}{S}\right)b}{0.5\left(\frac{K}{S}\right)f + \left(\frac{K}{S}\right)b} \tag{4}$$

where $(K/S)_b$ is the K/S value of the back face of the printed fabric, and $(K/S)_f$ is the K/S value of the front face of the printed fabric.

2.4.4. Colorfastness properties of printed fabric

Colorfastness to washing was conducted according to the colorfastness to domestic and commercial laundering ISO 105-C06:2010 using reference detergent type 1 (SDC, England) without optical brightening agent, DW (Diacetate-Wool) multifiber adjacent fabric, and following the test number A1S.

Furthermore, to understand the stability of the binder, colorfastness to laundering: Accelerated washing cycles were conducted following AATCC Test Method 61-2009. All the printed samples were subjected to 5 washing cycles that correspond to 25 typical careful hand launderings at a temperature of 40 ± 2 °C.

Colorfastness to rubbing (dry and wet conditions) was carried out by following ISO 105-X12:2016. Colorfastness to perspiration was conducted following AATCC Test Method 15–2009. The assessment of colorfastness to washing, rubbing, and perspiration was evaluated using the standard grey scale grading method. The samples were assessed on a scale of 1 to 5, where 1 indicates very poor fastness and 5 represents excellent performance.

The colorfastness to light test was conducted according to the ISO 105-B02:2014 lightfastness test method using the Light Fastness Tester (TruFade 1800, James Heal, UK) equipped with a xenon arc and mercury-tungsten fluorescent lamp. The change in color for the samples subjected to the lightfastness test was assessed by comparing the samples with the blue wool reference standard as specified in the ISO standard. Lightfastness of the printed samples was graded on a blue scale ranging from 1 to 8, where increasing values correspond to higher resistance to fading. Categorized in ascending order of quality, the levels are very poor, poor, moderate, fairly good, good, very good, excellent, and outstanding.

2.5. Scanning electron microscopy (SEM)

The surface morphology of the printed fabric was examined using field emission scanning electron microscopy (FE-SEM; Zeiss Sigma VP, Germany) equipped with an InBeam detector operated at an accelerating voltage of 20 kV. This analysis was carried out to evaluate the structural stability of the biobased binder formulation before and after repeated washing cycles. The washed and unwashed fabric specimens were mounted on aluminium stubs using adhesive carbon tape to ensure proper electrical contact. A thin layer of gold/palladium (80Au/20Pd) was sputter-coated (EM 600, Leica Microsystems, Wetzlar, Germany) onto the samples prior to imaging to enhance surface conductivity.

2.6. Fabric touch test for printed fabric using the fabric touch tester (FTT)

The tactile properties of printed fabric were evaluated using a Fabric Touch Tester device (SDLATLAS, USA), which provides an objective assessment of fabric hand. Since chitosan and cationic starch are known for their strong film-forming ability, which can increase fabric stiffness, the sample printed with 1% dye concentration (containing the highest relative biobased binder content) was selected for this analysis. Before the measurement, all the samples were carefully ironed to eliminate creases that might affect the results and then conditioned for 24 h under standard atmospheric conditions (65 ± 2% RH, 20 ± 2 °C). The samples were prepared according to the FTT manufacturer's guidelines in Wales direction orientation, referring to vertical columns of loops of the knitted fabric. In this study, the key sensorial comfort indices were assessed, focusing on smoothness, softness, and warmth, which represent key predictors of perceived fabric comfort. In addition, the two global comfort indices representing active (hand) and passive (touch) sensations were assessed for both outer and inner sides of the fabric. These indices, together with the primary ones, are normalized on the scale of 0 to 1 and then classified into five comfort grades: very low (1), low (2), middle (3), high (4), and very high (5) quality [33].

3. Results and discussion

3.1. Zeta potential and QCM-D measurements

Zeta potential measurements were conducted across a range of pH values for the dye, chitosan, cationic starch, and the formulated biobased binder to determine the optimal pH for the printing paste prior to printing trials. The pH plays a significant role in governing the electrostatic interactions between charged biomacromolecules by changing the ionization state of their functional groups. Chitosan exhibits a strongly positive zeta potential at acidic pH values due to the protonation of its primary amine groups [34], reaching approximately +48 mV at pH 3.5 (Fig. 1a). This value gradually declined with increasing pH and approached neutrality around pH 7.5–8, aligned with the known protonation constant (pK_a) of chitosan [35]. In contrast, sea buckthorn extract showed consistently negative zeta potential values at higher pH, suggesting the presence of deprotonated acidic moieties such as phenolic and carboxylic groups [36,37]. Cationic starch, on the other hand, showed a moderate positive charge throughout the pH range, with relatively stable zeta potential values between +20 mV and +10 mV, highlighting its cationic nature.

The biobased binder exhibited a distinct pH-dependent zeta potential, increasing from approximately +21 mV at pH 3 to a maximum of around +33 mV at pH 5, followed by a decrease at higher pH. This nonlinear trend can be related to the combined effects of polymer-polymer interactions and conformational rearrangements within the multicomponent binder system [38,39]. The increase in zeta potential value of the binder systems up to pH 5 suggests a higher positive surface charge and enhanced colloidal stability under these conditions.

Based on these observations, the optimal pH range for the printing paste formulation was identified between pH 4 and 5.5, where the charge contrast between the positively charged biobased binder and negatively charged sea buckthorn extract was maximized. Such charge difference promotes effective electrostatic interaction between the dye molecules, the cationic binder components, and the anionic cellulosic substrate, enhancing dye retention within the printing matrix [40]. Since the sea buckthorn dye showed maximum deprotonation at pH 5–5.5, and further lowering the pH would risk degrading the carotenoid-rich components, known to be sensitive to acidic conditions due to their chemical structure [41] pH 5 was selected as the optimum pH for printing paste preparation.

To investigate the interactions between the sea buckthorn dye and biopolymer-based binder on CNF, QCM-D measurements were conducted at pH 5. The sequential adsorption of biopolymers and dye on a CNF thin film-coated QCM sensor is shown in Fig. 1b. The changes in frequency (Δf) provide information regarding the adsorbed mass: negative shifts indicate higher mass uptake (adsorption), and positive shifts indicate mass loss (desorption).

On adsorption of chitosan and cationic starch at pH 5, the largest frequency decrease was observed for cationic starch, reflecting its higher affinity for the CNF-coated surface. After sensor stabilization at approximately 50 min, introduction of cationic starch led to a steep and

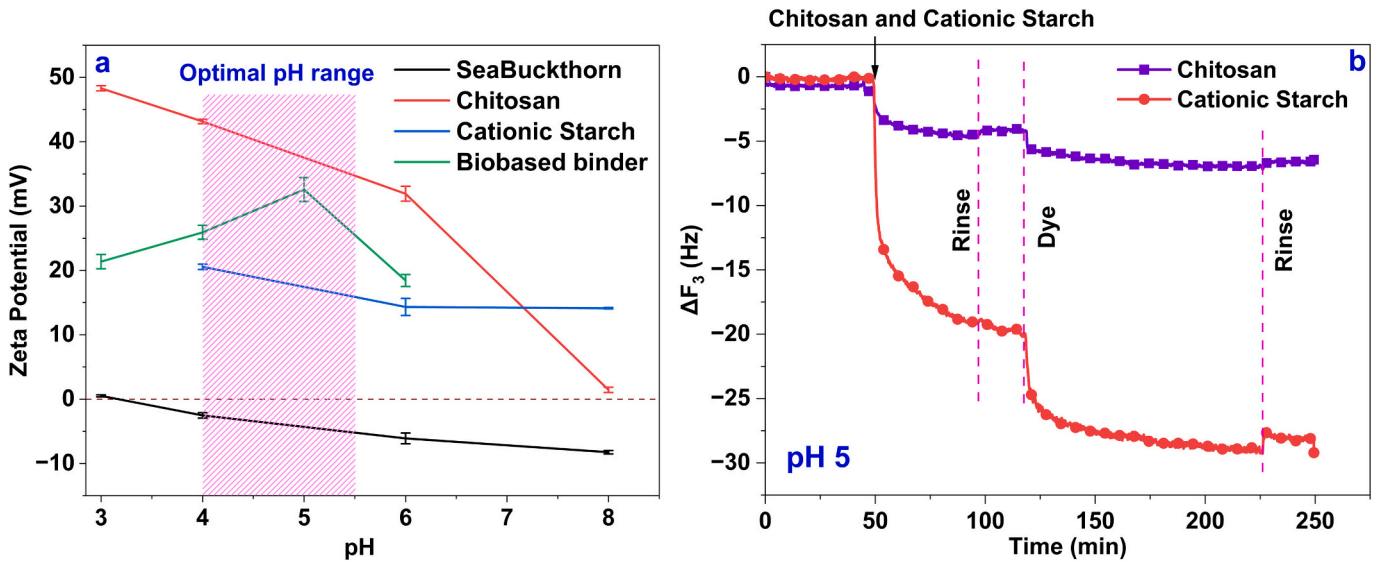

Fig. 1. (a) Zeta-potential measurements for sea buckthorn dye, chitosan, and cationic starch, and biobased binder across different pH ranges; (b) QCM-D adsorption change in oscillation frequency (3rd overtone) after injection of chitosan, cationic starch, and sea buckthorn dye.

immediate decline in frequency, suggesting rapid adsorption on the negatively charged CNF surface. This interaction can be attributed to the strong electrostatic attractions between the positively charged quaternary ammonium groups in cationic starch and the anionic carboxyl groups on the CNF surface [42]. Following the first rinsing step (at 100 min), the frequency remained relatively stable, indicating the formation of a stable cationic starch layer under the QCM-D rinsing conditions. Subsequent injection of the sea buckthorn dye solution produced a further decline in frequency (at 125 min), indicating dye adsorption facilitated by the pre-adsorbed cationic starch layer. The cationic starch likely promoted dye adsorption by providing additional binding sites and enabling secondary interactions such as van der Waals forces [43,44]. The final rinsing step (at 225 min) caused only slight desorption of loosely bound dye molecules, suggesting that a substantial fraction of the adsorbed material remained associated with the model CNF surface.

For comparison, the adsorption of chitosan on the CNF-coated surface at pH 5 was moderate relative to cationic starch. Based on the Sauerbrey equation, the adsorbed mass of chitosan was approximately 38 ng/cm^2, compared with 164 ng/cm^2 for cationic starch (Fig. S1). This is likely due to a lower fraction of protonated amine groups in chitosan at this pH, leading to electrostatic attraction to the negatively charged CNF [45]. Furthermore, chitosan's relatively rigid and semi-crystalline structure, together with possible intermolecular association in solution, can limit chain spreading and reduce the amount of polymer adsorbed [46]. Chitosan typically exhibits stronger adsorption at lower pH (around 4), where amine groups are nearly fully protonated. However, in our system, we balanced dye stability and functionality with polyelectrolyte protonation. Despite its moderate adsorption at pH 5, the chitosan layer remained stable after rinsing, suggesting firm binding via electrostatic interactions [39]. Together with the zeta-potential results, these observations support the proposed interfacial interactions among the binder components, dye, and cellulosic surface under the selected formulation conditions. However, the QCM-D measurements represent adsorption behavior on a model CNF surface and were not used to establish a quantitative relationship between interfacial adsorption and the colorfastness of the printed textiles.

3.2. *Rheological and thermal properties of binder formulation and printing pastes*

The shear-dependent viscosity and shear stress behavior of the biobased binder and synthetic binder, along with their dye-containing formulations, were evaluated for screen-printing suitability. All samples exhibited shear-thinning behavior, which is highly desirable for screen printing pastes. Viscosity (η) versus shear rate (γ) and shear stress (τ) versus shear strain rate curves are presented in Fig. 2a, b. The increase in viscosity at low shear prevents paste spreading on the screen, while a rapid decrease in viscosity at high shear facilitates smooth flow through the mesh [47,48]. After passing through the mesh, the ink should rapidly recover its structural integrity and elasticity to maintain sharp and uniform print patterns and avoid slumping or deformation [49].

The biobased binder formulations (Fig. 2a) showed a stable, clear shear-thinning profile consistent with pseudoplastic fluids. The viscosity values, even at lower shear rates (0.01s^{-1}), were within the optimal range reported for textile printing pastes [50–52]. This suggests that the biobased binder possesses suitable flow and film-forming characteristics for screen printing applications. Incorporation of natural dye slightly altered the flow behavior but preserved the overall shear-thinning trend, confirming good compatibility between the sea buckthorn dye and the biopolymer matrix.

The shear stress and shear rate relationships for the biobased binder, the synthetic binder, and their dye-containing formulations show a non-linear increase in shear stress value with increasing shear rate, confirming the non-Newtonian behavior of the biobased binder system (Fig. 2b). Moreover, the smooth stress response across the shear range demonstrates structural stability and good recovery behavior, which are critical attributes for achieving sharp, uniform prints; this aspect is examined further in Section 3.7. Overall, these results confirm that the biobased binder exhibits rheological characteristics suitable for textile printing applications.

Thermogravimetric analysis (TGA) was performed to evaluate the thermal stability and decomposition profiles of the biobased binder, its sea buckthorn dye-loaded formulation, sea buckthorn dye alone, and the PU-based synthetic binder (Fig. 2c). This is crucial for assessing the suitability of the biobased binder in textile applications, particularly under processing conditions involving heat, such as drying and curing steps.

A notable difference in the thermal stabilities between the samples could be observed from the thermograms and the corresponding derivative (DTG) curves (Fig. 2d). The biobased binder exhibits an initial mass loss between 35 °C and 125 °C, attributed to the removal of free and bound water [53]. As reported in earlier studies, dehydration is not considered to affect the thermal degradation of biobased binder

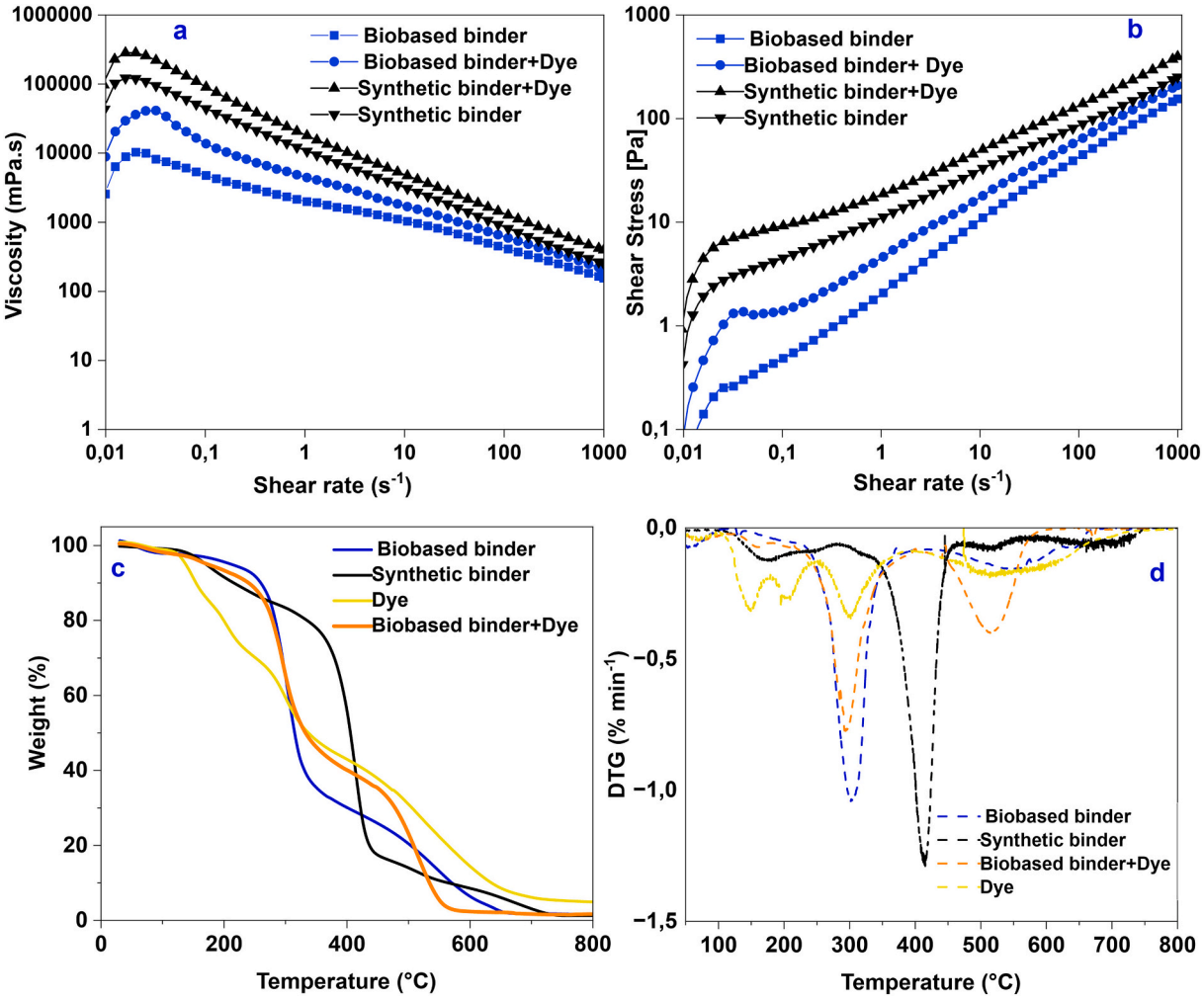

Fig. 2. (a) Viscosity (η) vs shear rate (γ) curves and (b) shear rate(γ) vs shear stress (τ) curves for comparison of biobased binder and synthetic binder properties, (c) TGA and (d) DTG curves of biobased binder, synthetic binder, and their dye-containing formulations.

constituents [54,55]. A second mass loss between 125 and 190 °C can be associated with glycerol decomposition [56]. The third stage began above 245 °C, corresponding to the chemical degradation of glycosidic bonds in cationic starch and chitosan [57,58].

On the other hand, sea buckthorn dye shows an initial mass loss below 130 °C, attributable to the evaporation of residual moisture, followed by secondary loss beginning around 180 °C associated with thermal cleavage of labile functional groups in carotenoid and flavonoid compounds. The major mass loss occurred between 200 and 300 °C, reflecting thermal degradation of phenolic and flavonoid compounds [59]. Interestingly, when the dye is incorporated into the biobased binder matrix, the onset of substantial formulation degradation remains above 250 °C, indicating that the polysaccharide network provides a protective environment for the dye molecules [60,61]. This stability is particularly relevant here, since the sample curing is conducted at 160 °C, which is well below the decomposition threshold. This ensures that the dye retains its structural integrity and functional properties during the curing process.

As expected, the PU-based synthetic binder exhibits higher thermal stability than the biobased binder. Its initial mass loss begins around 225 °C, which could be attributed to the breakdown of urethane linkages [62]. A second region was observed between 350 and 400 °C, associated with thermal degradation of the PU hard segments [63]. The final weight loss observed between 355 and 440 °C is related to the hydrocarbon chain decomposition of polyester amide polyols [64].

3.3. Toxicity analysis of sea-buckthorn dye

Sea buckthorn dye exhibited concentration-dependent effects across cell viability, cytotoxicity, oxidative stress, and skin sensitization assays (Fig. 3), with pronounced responses at the highest concentration of 1.0 mg/mL. In the MTT assay, cell viability decreased by 47% at 1.0 mg/mL versus control ($p < 0.001$), and a similar decrease was observed in the PI-digitonin assay (Fig. 3a). Consistently, this cytotoxic effect was further supported by an increase in lactate dehydrogenase (LDH) release into the cell-free culture medium that increased by 1.8-fold at 1.0 mg/mL ($p < 0.01$) versus control (Fig. 3b).

The oxidative stress response normalized to total cell number (Fig. 3c, d) demonstrated a 7.4-fold increase in mitochondrial superoxide production (MitoSOX assay, $p < 0.001$) (Fig. 3c), and a 12.4-fold increase was found in intracellular ROS production ($p < 0.0001$) at 1.0 mg/mL of extract compared to the control (Fig. 3d). This indicates that the extract can elevate oxidative stress reactions at this concentration.

From the skin sensitization assay outcomes (Fig. 3e, f), a marked reduction in keratinocyte viability (approximately 80%) was observed at the two highest extract concentrations. Nevertheless, no reporter gene induction was detected at any concentration despite the cytotoxicity, indicating no skin-sensitizing potential under the tested conditions for the sea buckthorn extract. However, this should be confirmed with another sensitization assay to validate results, as recommended by OECD guidelines [27]. Overall, to produce unfavorable effects in HepG2 cells, high dye concentrations were needed, suggesting that the extract

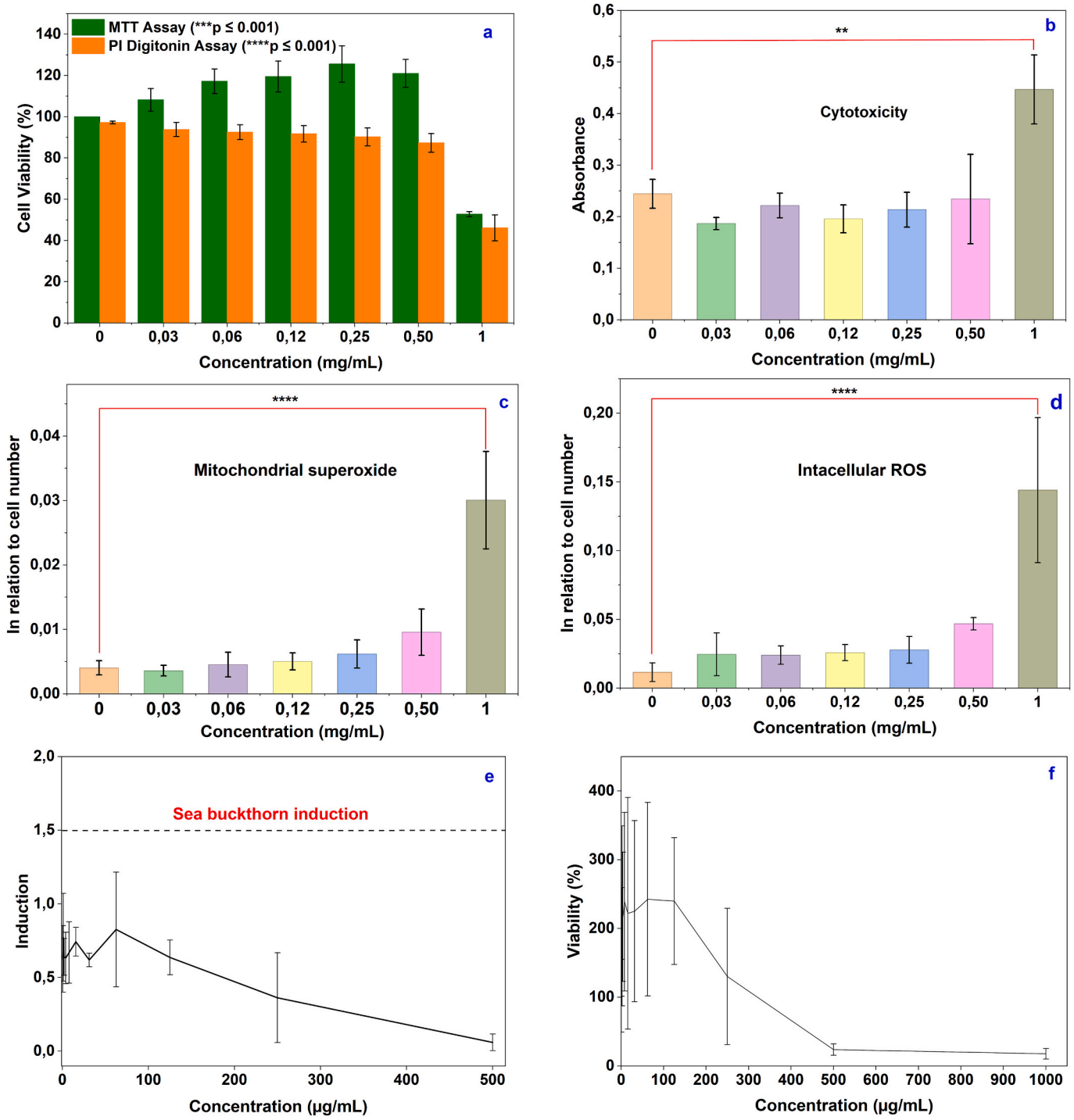

Fig. 3. Effect of 24-hour exposure to sea buckthorn extract on cell viability and cytotoxicity in human hepatic HepG2 cells: (a) MTT and PI-digitonin assay, (b) LDH assay; Oxidative stress responses following 24-hour exposure, showing (c) mitochondrial superoxide production (MitoSOX assay), (d) intracellular reactive species (ROS) levels; Skin sensitization assessment after 48 -hour exposure, presenting (e) reporter gene induction relative to control, with the 1.5-fold induction threshold indicated by a dashed line, and (f) corresponding cell viability. Data are expressed as mean ± SD (n = 3–6 for viability and cytotoxicity assays; n = 3 for oxidative stress and skin sensitization assays). Statistical significance is indicated by $^{**}p \leq 0.01$; $^{***}p \leq 0.001$; $^{****}p \leq 0.0001$.

has potential as a natural colorant, although further studies are needed to verify its safety profile. Following these in vitro findings, we also conducted perspiration-fastness testing, as described in detail in Section 3.6, the results of which supported a low dermal exposure scenario during wear.

In this study, toxicity assessment was conducted only for the sea buckthorn dye, as it is the primary component with potential biological activity. The biobased binder components, chitosan, cationic starch, and glycerol, are well-established, renewable, biodegradable, and widely regarded as biocompatible polymers, with extensive prior use in biomedical, pharmaceutical, and textile applications [65–67]. Therefore, based on their well-documented safety profiles, no additional toxicity tests were conducted for these constituents in this work.

3.4. Antibacterial assessment

The antibacterial performance of untreated, printed, and washed cotton textiles was evaluated against the luminescent *E. coli* and *S. aureus* using an imaging assay after overnight incubation (Fig. 4). The assay enables visualization and quantification of bacterial metabolic activity directly on textile surfaces, providing information on localized antibacterial effects following longer exposure.

The antimicrobial activities of the biobased binder and sea buckthorn dye were assessed individually to determine their respective contributions to the antibacterial performance of the printed textiles. Both materials exhibited antibacterial effects, with responses depending on bacterial strain and concentration (Fig. S2). The biobased binder showed consistent inhibition against both strains and reached over 60% inhibition against *S. aureus* at the highest concentration. Sea buckthorn dye was particularly active against *E. coli*, while a concentration-dependent adaptive response was observed for *S. aureus*. Real-time luminescence monitoring confirmed strain-dependent differences in bacterial response and revealed transient metabolic adaptation at higher dye concentrations (Fig. S3).

Against *E. coli* (Fig. 4a), untreated cotton exhibited negative inhibition values, indicating higher luminescence relative to the bacterial control. This response suggests that untreated fabric may support bacterial metabolic activity by retaining moisture or providing attachment sites. Cotton printed with the biobased binder alone also yielded negative inhibition, indicating limited antibacterial efficacy under these conditions. In contrast, cotton printed with the sea buckthorn dye and biobased binder showed clear 5–20% inhibition, which declined slightly after 25 washing cycles, demonstrating partial retention of antibacterial effect.

Against *S. aureus* (Fig. 4b), all textile samples exhibited higher antibacterial activity than against *E. coli*. Untreated cotton showed some inhibition, possibly due to residual textile treatment chemicals with activity against the Gram-positive bacteria, and biobased binder-printed cotton showed low or negative inhibition. The sea buckthorn biobased binder–printed sample exhibited the strongest antibacterial activity, reaching 45–50% inhibition, with a slight reduction after repeated washing.

The differences between the two bacteria align with known structural and physiological distinctions between Gram-negative and Gram-positive species. The greater sensitivity of *S. aureus* may be attributed to the absence of an outer membrane, which generally makes Gram-positive bacteria more susceptible to surface-associated antibacterial compounds. In contrast, the outer membrane of *E. coli* likely provides greater resistance to antibacterial substances immobilized on or released from textile surfaces. Similar behavior has been reported for cellulose fabrics and hand sheets [29,68]. Kunnas et al. [69] also observed high activity against *S. aureus* but only moderate activity against *E. coli* in Jacquard textiles treated with micro-encapsulated supercritical carbon dioxide extracts of *Angelica archangelica* and *Rhododendron tomentosum*. The reduced efficacy observed after washing, particularly for the sea buckthorn–treated cotton, suggests that at least part of the antibacterial activity arises from weakly bound or surface-associated compounds that are susceptible to removal during laundering. Background effects from finishing agents or processing residues in untreated cotton may also influence the baseline antibacterial or growth-supporting behavior, which was reduced after washing. Efficiency further depends on antibacterial agent dose and mode of action when considering the test method suitability [29,31,70].

Overall, the imaging-based assay following overnight incubation highlights clear strain-dependence and treatment-specific antimicrobial effects on cotton textiles. The results emphasize the importance of considering washing stability and textile background effects when evaluating the antimicrobial performance of bio-based textile treatments.

3.5. Color parameters of the printed textiles

The color strength (K/S) values of the printed fabrics varied significantly depending on the choice of the binder and the dye concentration (Table 2). Increasing the dye concentration from 1% to 3% and 5% for both biobased binder and synthetic binder systems resulted in greater K/S values, indicating better surface coloration with higher loading. The samples printed with a biobased binder exhibited notably higher K/S values compared to those with a synthetic binder at matched dye concentrations. This suggests that the biobased binder leads to more effective dye-fiber interaction and better pigment fixation. At 3% dye concentration, the K/S value of the biobased binder printed samples reached 3.07 ± 0.24 compared to 1.53 ± 0.09 for the synthetic binder, while at 5% dye concentration, the biobased formulations achieved a K/S of 4.15 ± 0.35.

This superior color yield in biobased formulations can be attributed to chitosan and cationic starch, whose protonated amino and quaternary ammonium groups promote electrostatic interaction with anionic polyphenolic dye molecules, enhancing dye retention within the printed fabric. Such strong electrostatic binding is widely known as the dominant mechanism governing dye adsorption in cationic polymer systems [42,71,72]. Beyond electrostatic binding, hydrogen bonding and cation-π interactions with aromatic dye molecules, along with reduced dye aggregation in the cationic polysaccharide matrix, can enhance apparent chromatic intensity [73]. The CIELAB results further support these findings, as fabrics printed with biobased formulation showed lower L* (darker shades) and slightly higher a* and b* values with increasing dye concentration.

Ink penetration plays an important role in textile printing, as it influences how ink diffuses through the fabric structure. Generally, higher

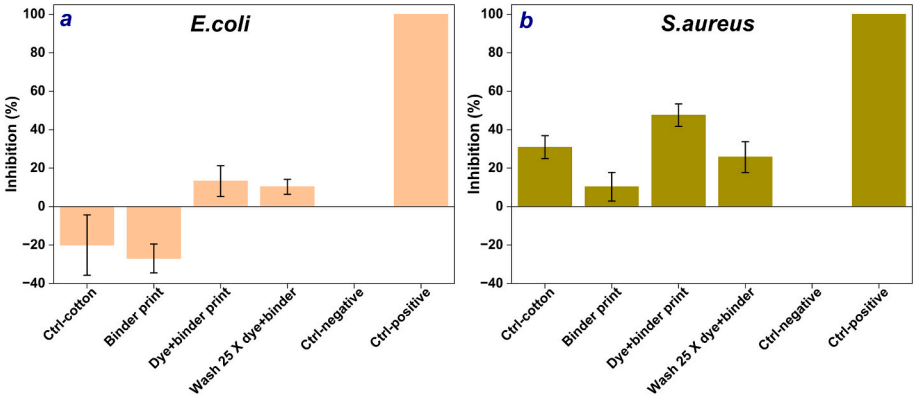

Fig. 4. Antibacterial inhibition of untreated, printed, washed cotton samples and the negative and positive controls against (a) *E. coli* and (b) *S. aureus* in the imaging assay. Results are shown as means ± standard deviation of three replicates in separate 6-well plates.

Table 2
K/S, L*a* b* values, and Ink penetration of printed cotton fabrics.

Sample	K/S	Ink penetration (%)	L*	a*	b*	Spectrophotometer image
$BB_{1\%}$	0.71±0.05	44	82.05	4.07	22.02	
$BB_{3\%}$	3.07±0.24	35	60.54	9.21	23.73	
$BB_{5\%}$	4.15±0.35	36	56.90	9.50	24.69	
$SB_{1\%}$	0.64±0.08	39	86.06	1.91	20.95	
$SB_{3\%}$	1.53±0.09	28	77.64	4.70	28.26	
$SB_{5\%}$	1,73±0.13	21	69.34	4.54	14.27	

ink penetration indicates greater ink diffusion through the fabric structure, which may result in reduced color intensity in printed fabric. Consistent with this, samples printed with lower dye concentration exhibited higher ink penetration and correspondingly smaller K/S values, indicating reduced surface color yield. This inverse relationship between ink penetration and color strength agrees with previous observations on cotton [32]. Notably, both the biobased and synthetic binders produced comparable ink penetration behavior. Overall, the biobased binder promotes efficient color fixation and uniform layer formation while maintaining optimal ink penetration suitable for textile printing applications with natural dyes.

3.6. Colorfastness assessment

The wash fastness testing showed excellent color stability for both the biobased and synthetic binder systems (Table 3). After a single wash, all samples achieved good-to-excellent (4/5) color-change ratings and no staining on adjacent multifiber fabrics (grey scale grade 5), indicating strong dye fixation and binder-fiber interactions. After 5 accelerated washing cycles, equivalent to 25 typical careful hand launderings at 40 ± 2 °C [74], color change decreased slightly, while staining grades remained unchanged. Notably, the biobased binder maintained comparable performance with the synthetic binder even after repeated washing cycles, confirming resistance to washing-induced dye removal. Overall, these results demonstrate durable color fixation suitable for repeated laundering, making the biobased binder a promising alternative for natural-dye textile printing.

Lightfastness testing revealed moderate to low resistance to photofading. Higher dye concentrations showed slightly reduced lightfastness (blue scale grading 2–3) for both biobased and synthetic binders, whereas lower dye concentrations performed marginally better (blue scale 4). This decline with increasing dye concentration aligns with the inherent photodegradation nature of bio-based dyes. Sea buckthorn dye is rich in carotenoids, including β-carotene, lycopene, zeaxanthin, and lutein, as well as phenolic compounds such as flavanol glycosides, catechins, and phenolic acids [75]. These compounds contain highly conjugated chromophores that impart a characteristic yellow color but are also prone to photo-oxidation under prolonged UV exposure. In particular, carotenoids can easily undergo oxidation, isomerization, and chain cleavage, which results in fading [76]. These reactions disrupt the chromophoric structures and lead to color fading. At higher loadings, excess dye molecules that are not strongly adhered to the polymer matrix remain exposed on the surface, where they degrade faster. Therefore, the moderate light fastness observed is consistent with the known photodegradation behavior of sea-buckthorn-derived dyes. The lightfastness of natural dyes may be improved by incorporating biobased UV-absorbing or antioxidant additives, such as lignin- or tannin-based compounds, or by protecting the colorants through microencapsulation or surface coating [77]. UV-absorbing additives can offer a relatively simple formulation-based approach but may affect paste rheology, shade, and color strength. Microencapsulation may provide a stronger barrier against light and oxygen but can increase formulation complexity and influence dye release, fixation, and fabric handle [41,78]. Further optimization should therefore include screening compatible UV absorbers and antioxidants, evaluating encapsulated sea buckthorn colorants, and assessing their effects on printability, color strength, shade, tactile properties, and lightfastness under standardized accelerated exposure.

Rubbing fastness of both binders was excellent in both wet and dry conditions (grey scale 4–5). Although wet rubbing fastness is typically one grade lower than dry rubbing fastness due to increased dye mobility in the presence of moisture [79] both binders maintained consistently high performance in wet and dry rubbing conditions. This suggests a strong adhesion between the dye-binder complex and the textile substrate. For the biobased binder-printed samples, the chitosan-cationic starch matrix likely forms a cohesive polymeric film that effectively encapsulates dye molecules, minimizing surface migration during mechanical abrasion.

The perspiration fastness results showed excellent resistance to color change and staining for both biobased and synthetic binder systems (Table 3). All printed samples achieved a grey scale grading of 4/5 for color change and 5 for staining on adjacent fabrics, regardless of dye concentration. This result confirms that the printed fabrics maintained color integrity with minimal dye migration under acidic conditions. Given that the cytotoxic effects on keratinocytes occurred only at high concentrations, the perspiration test results provide complementary evidence for a low dermal exposure scenario. Accordingly, dermal exposure to the sea buckthorn dye from the printed textiles is expected

Table 3
Color fastness of printed samples.

Sample	Washing (change in color) single*	Washing (change in color) multiple**	Rubbing dry	Rubbing wet	Light	Perspiration (change in color)
$BB_{1\%}$	4/5	3/4	5	4/5	4	4/5
$BB_{3\%}$	4/5	3/4	5	4/5	2	4/5
$BB_{5\%}$	4/5	3/4	5	4	2	4/5
$SB_{1\%}$	4/5	3/4	5	5	4	4/5
$SB_{3\%}$	4/5	3/4	5	5	2	4/5
$SB_{5\%}$	4/5	3/4	5	5	3	4/5

*Single wash; ** Five accelerated washes equal to 25 washes. Staining on wool, acrylic, polyester, polyamide, cotton, and diacetate was grade 5 for all samples for wash (single and multiple washes) and perspiration fastness in a grey scale grading.

to be very low, supporting the printed fabric's suitability for skin-contact applications under tested conditions.

3.7. SEM imaging and print sharpness

The surface morphology of the printed samples was examined using FESEM to investigate the stability of the printed samples after repeated washing cycles. The biobased binder-printed fibers exhibited a thin, uniform surface coating, indicating good initial adhesion (Fig. 5a). After one wash, the coating remained largely intact, with only minor surface irregularities (Fig. 5b), consistent with strong interaction between the biobased binder components and the fiber. Even after five repeated washing cycles, fibers retained the paste, although localized erosion was observed (Fig. 5c). This result is in line with the washing fastness gradings (Table 3). The synthetic binder printed samples showed a more continuous and smoother film surface (Fig. 5d), as expected for a PU-

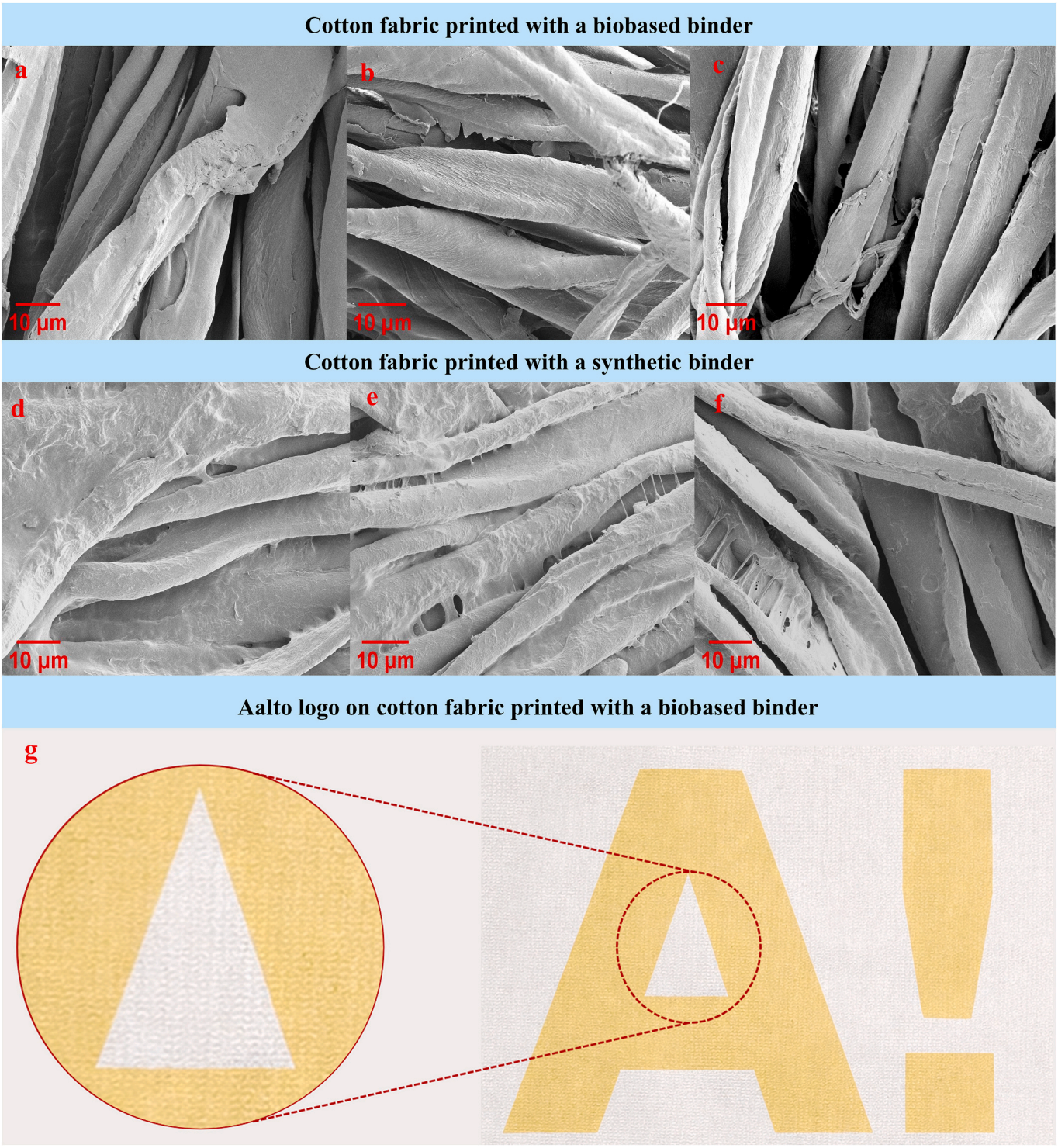

Fig. 5. SEM images of cotton fabrics before and after washing: Sample (a) printed with biobased binder, (b) after 1 wash, (c) after 5 accelerated washes; Sample (d) printed with synthetic PU binder, (e) after 1 wash, and (f) after 5 accelerated washes; (g) Visual print sharpness assessment of Aalto University logo printed with biopaste.

based synthetic binder. After one washing cycle, no huge changes were observed on the surface (Fig. 5e), indicating minimal disruption even after five consecutive cycles (Fig. 5f). Overall, the SEM observations support the washing fastness results, demonstrating that the biobased binder provides washing resistance comparable to the synthetic PU binder.

In addition to wash durability, the printing quality of the developed biobased binder was evaluated by examining the printed pattern's edge sharpness and definition. The printed logo exhibited well-defined edges and a uniform color distribution across the printed area (Fig. 5g**)**. The magnified region, the triangular inner section of the letter "A", shows distinct boundaries between printed and unprinted fabric areas with minimal edge feathering or dye migration, indicating controlled paste spreading and excellent rheological behavior of the printing paste. The absence of spreading reflects sufficient viscosity and shear-thinning behavior to allow the paste to transfer cleanly through the screen. As a result, the biobased binder enabled controlled paste deposition and high print resolution.

3.8. Sensorial properties of printed fabric

The sensorial properties of fabrics printed with biobased binder were evaluated using FTT to assess the influence of the binder composition on the tactile performance, which is an end-use critical parameter for textile applications. Several parameters govern the hand-feel of a printed fabric, including surface morphology, printed layer flexibility, and the structural characteristics of the binder components [80].

The sensorial properties of fabrics printed with biobased binder showed hand-feel comparable to synthetic binder prints (Table 4**)**. Smoothness was similar in active and passive modes with FTT grades of 4, indicating consistently smooth surfaces regardless of the binder type. Softness assessments also matched, as both binders achieved the same FTT grades of 3–4, indicating minimal perceptible difference to human touch. Warmth perception was comparable as well, receiving grade 3 for both, aligning with their similar thermal and surface characteristics.

These observations can be attributed to the structural behavior of the biopolymer components of the binder. Both chitosan and cationic starch are semi-crystalline polysaccharides [81]. However, when blended together, their native crystalline regions can be partially disrupted due to intermolecular interactions, resulting in increased chain mobility and enhanced flexibility of the material, as reported in previous studies [82,83]. Moreover, heat treatment can also induce changes in the crystallinity of the binder components, and the presence of glycerol in the binder formulation as a plasticizer promoted the disruption of native crystalline polymer chains by forming hydrogen bonds with cationic starch during processing [84].

Overall, these findings demonstrate that the biobased binder offers tactile properties equivalent to that of the synthetic binder used in this study, supporting its suitability for clothing applications where hand-feel is crucial.

4. Conclusion

We developed a biobased binder formulation composed of chitosan, cationic starch, and glycerol that performs effectively with a sea buckthorn-derived natural dye for textile screen printing. The paste exhibited strong shear-thinning and rapid structural recovery, enabling smooth mesh flow and sharp, uniform patterns. Printed fabrics exhibited excellent wash durability, retaining color even after 5 accelerated laundering cycles, and FESEM confirmed a stable biopolymer film on the fiber surface, with strong binder-fiber adhesion and minimal surface degradation. The biobased system also provided antimicrobial functionality, with both the biobased binder and sea buckthorn dye inhibiting *E. coli* and *S. aureus* without additional antimicrobial agents. Importantly, in vitro testing indicated no skin sensitization potential for the sea buckthorn dye under the conditions used. Also, Fabric Touch Tester measurements showed tactile properties like smoothness, flexibility, and overall hand feel, comparable to those of a PU-based synthetic binder.

Overall, the present study shows the successful development of a biobased binder for natural dye printing with suitable rheological and printing characteristics, good wash durability and print definition, and satisfactory tactile performance. However, its broader environmental and industrial performance requires further investigation. Future work should therefore address lightfastness optimization, long-term storage stability, scale-up and process economics, and extended antibacterial durability under washing, abrasion, and perspiration. Comprehensive toxicological assessment of printing effluents and quantitative environmental assessment in comparison with conventional binder systems should also be considered to support further development and evaluation of the proposed formulation for practical natural-dye textile printing applications.

CRediT authorship contribution statement

Ritesh Sharma: Writing – review & editing, Writing – original draft, Visualization, Methodology, Investigation, Formal analysis, Data curation, Conceptualization. **Mikko Herrala:** Writing – review & editing, Writing – original draft, Validation, Formal analysis, Data curation. **Jenni Tienaho:** Writing – review & editing, Writing – original draft, Investigation, Data curation. **Riikka Haapala:** Writing – original draft, Investigation. **Jaana Rysä:** Writing – review & editing, Methodology. **Ali Tehrani-Bagha:** Writing – review & editing, Supervision, Project administration, Funding acquisition, Conceptualization. **Paula Nousiainen:** Writing – review & editing, Writing – original draft, Supervision, Resources, Project administration, Methodology, Funding acquisition, Formal analysis, Conceptualization.

Declaration of Generative AI and AI-assisted technologies in the writing process

Aalto University's AI assistant tool was used to improve the language and readability of the manuscript. After using this tool, the authors reviewed and edited the content as needed and take full responsibility for the content of the publication.

Table 4
FTT-based evaluation of primary and global comfort indices (mean ± standard deviation) and FTT grading.

Property	Evaluation mode	Biobased binder (index)	Biobased binder FTT grading	Synthetic binder (index)	Synthetic binder FTT grading
Smoothness	Hand (active)	0.63 ± 0.15	4	0.64 ± 0.09	4
	Touch (passive)	0.72 ± 0.05	4	0.76 ± 0.07	4
Softness	Hand (active)	0.64 ± 0.13	4	0.67 ± 0.07	4
	Touch (passive)	0.53 ± 0.04	3	0.55 ± 0.07	3
Warmth	Hand (active)	0.48 ± 0.16	3	0.44 ± 0.13	3
	Touch (passive)	0.37 ± 0.01	3	0.32 ± 0.01	3
Total comfort	Hand (active)	0.59 ± 0.07	4	0.60 ± 0.03	4
	Touch (passive)	0.59 ± 0.03	4	±0.06	4

Funding sources

We acknowledge the financial support for this study from the Research Council of Finland's Flagship Program under Projects No. 369114 and 369115 (Competence Center for Materials Bioeconomy, FinnCERES) and Strategic Research Council at Research Council of Finland (352466, Biobased Dyes abd Pigments for Color Palette) project.

Declaration of competing interest

The authors declare that they have no known competing financial interests or personal relationships that could have appeared to influence the work reported in this paper.

Acknowledgements

Ulla Jauhiainen is thanked for proficient laboratory work with antibacterial tests at Luke Laboratories. The University of Helsinki Biomedicum Imaging Unit (BIU) is acknowledged for the opportunity to use the Lago in vivo imaging system to obtain in vivo bacterial imaging data.

Appendix A. Supplementary data

Supplementary data to this article can be found online at https://doi.org/10.1016/j.porgcoat.2026.110630.

Data availability

Data will be made available on request.

References

[1] J. Sharma, S. Sharma, V. Soni, Classification and impact of synthetic textile dyes on aquatic flora: a review, Reg. Stud. Mar. Sci. 45 (2021) 101802, https://doi.org/10.1016/j.rsma.2021.101802.
[2] T.A. Aragaw, A review of dye biodegradation in textile wastewater, challenges due to wastewater characteristics, and the potential of alkaliphiles, J. Hazard. Mater. Adv. 16 (2024) 100493, https://doi.org/10.1016/j.hazadv.2024.100493.
[3] J. Lin, W. Ye, M. Xie, D.H. Seo, J. Luo, Y. Wan, B. Van Der Bruggen, Environmental impacts and remediation of dye-containing wastewater, Nat. Rev. Earth Environ. 4 (2023) 785–803, https://doi.org/10.1038/s43017-023-00489-8.
[4] J. Jiang, Y. Shen, D. Yu, M. Wu, L. Yang, S. Li, Sustainable washing-free printing of disperse dyes on polyester fabrics enabled by crosslinked fluorosilicone modified polyacrylate binders, Polym. Adv. Tech. 32 (2021) 641–650, https://doi.org/10.1002/pat.5117.
[5] K. Xie, A. Gao, M. Li, X. Wang, Printing properties of the red reactive dyes with different number sulfonate groups on cotton fabric, Carbohydr. Polym. 101 (2014) 666–670, https://doi.org/10.1016/j.carbpol.2013.09.107.
[6] E. Abd-Elaziz, Multipurpose pigment printing and functional finishing of cellulosic fabrics, Color. Technol. 140 (2024) 843–857, https://doi.org/10.1111/cote.12742.
[7] Md.R. Repon, B. Dev, M.A. Rahman, S. Jurkonienė, A. Haji, Md.A. Alim, E. Kumpikaitė, Textile dyeing using natural mordants and dyes: a review, Environ. Chem. Lett. 22 (2024) 1473–1520, https://doi.org/10.1007/s10311-024-01716-4.
[8] C. Li, H. Xiao, X. Wang, T. Zhao, Development of green waterborne UV-curable vegetable oil-based urethane acrylate pigment prints adhesive: preparation and application, J. Clean. Prod. 180 (2018) 272–279, https://doi.org/10.1016/j.jclepro.2018.01.193.
[9] T. Harifi, M. Montazer, Past, present and future prospects of cotton cross-linking: new insight into nano particles, Carbohydr. Polym. 88 (2012) 1125–1140, https://doi.org/10.1016/j.carbpol.2012.02.017.
[10] A. Hu, H. Peng, M. Li, S. Fu, Preparation of melamine-formaldehyde encapsulated fluorescent dye dispersion and its application to cotton fabric printing, Color. Technol. 135 (2019) 103–110, https://doi.org/10.1111/cote.12379.
[11] T. Bechtold (Ed.), Handbook of Natural Colorants, Repr, Wiley, Chichester, 2010.
[12] A. Kumar, A. Konar, Dyeing of textiles with natural dyes, in: E. Akcakoca Kumbasar (Ed.), Natural Dyes, InTech, 2011, https://doi.org/10.5772/21341.
[13] B. Patel, P. Kanade, Sustainable dyeing and printing with natural colours vis-à-vis preparation of hygienic viscose rayon fabric, Sustain. Mater. Technol. 22 (2019) e00116, https://doi.org/10.1016/j.susmat.2019.e00116.
[14] J. Wu, B. Li, P. Du, X. Xin, Z. Cai, F. Ge, A novel colored chitosan-modified polystyrene composite dye nanospheres with enhanced coloring properties for binder-free printing, Dyes Pigments 232 (2025) 112506, https://doi.org/10.1016/j.dyepig.2024.112506.
[15] L. Wang, S. Cui, H. Ni, M. Wu, W. Wang, New washing-free printing binder based on organosilicon-modified polyacrylate for polyester fabric printing of disperse dyes, Prog. Org. Coat. 123 (2018) 75–81, https://doi.org/10.1016/j.porgcoat.2018.06.009.
[16] W. Cheng, L. Pei, M.A. Saleem, L. Zhu, J. Wang, Sustainable pilot scale disperse dyeing in a waterless silicone medium dyeing system for no discharge of wastewater, J. Clean. Prod. 321 (2021) 128953, https://doi.org/10.1016/j.jclepro.2021.128953.
[17] Y.-Y. Zhu, C.-L. Cui, J.-Q. Xue, M.-W. Shi, Z.-H. Xu, W. Jiang, R. Wang, J.-J. Long, The adsorption behavior and phase transfer catalytic fixation of a special dye SCF-AOL2 on cotton in supercritical carbon dioxide, J. Supercrit. Fluids 188 (2022) 105651, https://doi.org/10.1016/j.supflu.2022.105651.
[18] J. Zhu, L. Pei, W. Niu, Q. Zhang, Z. Wu, J. Wang, An energy-efficient and water-saving alternative to conventional thermofixation: polydimethylsiloxane-mediated disperse dyeing of polyester, J. Environ. Chem. Eng. 14 (2026) 124512, https://doi.org/10.1016/j.jece.2026.124512.
[19] F. Ahmed, Md.R. Repon, A.D. Pranta, Md.S. Ragib Yasar, Md.F. Rakib, I. Ahmed, T. A. Emon, T.A. Nishat, Eco-sustainable printing of cellulosic polymeric material using bio-colorants and bio-crosslinkers, SPE Polym. 6 (2025), https://doi.org/10.1002/pls2.10159.
[20] M. Wennman, A.C. Pinon, A.J. Svagan, M. Hellberg, M.S. Hedenqvist, A biobased binder of carboxymethyl cellulose, citric acid, chitosan and wheat gluten for nonwoven and paper, Carbohydr. Polym. 323 (2024) 121430, https://doi.org/10.1016/j.carbpol.2023.121430.
[21] M. Wennman, M. Hellberg, A.J. Svagan, M.S. Hedenqvist, A biobased binder of emulsion type that provides unique and durable wet strength and hydrophobicity to paper and nonwoven, Ind. Crop. Prod. 193 (2023) 116126, https://doi.org/10.1016/j.indcrop.2022.116126.
[22] G. Sauerbrey, Verwendung von Schwingquarzen zur Wägung dünner Schichten und zur Mikrowägung, Z. Physik. 155 (1959) 206–222, https://doi.org/10.1007/BF01337937.
[23] P.V. Dludla, B. Jack, A. Viraragavan, C. Pheiffer, R. Johnson, J. Louw, C.J. F. Muller, A dose-dependent effect of dimethyl sulfoxide on lipid content, cell viability and oxidative stress in 3T3-L1 adipocytes, Toxicol. Rep. 5 (2018) 1014–1020, https://doi.org/10.1016/j.toxrep.2018.10.002.
[24] M. Herrala, J. Yli-Öyrä, A.F. De Albuquerque, N.O. De Farias, D.A. Morales, R. Räisänen, H.S. Freeman, G.A. Umbuzeiro, J. Rysä, Waterless dyeing and in vitro toxicological properties of biocolorants from *Cortinarius sanguineus*, J. Fungi (Basel, Switzerland) 8 (2022) 1129, https://doi.org/10.3390/jof8111129.
[25] J. Yli-Öyrä, M. Herrala, H. Kovakoski, E. Huuskonen, P. Toukola, R. Räisänen, J. Rysä, In vitro toxicity assessment of *Cortinarius sanguineus* anthraquinone aglycone extract, J. Fungi (Basel, Switzerland) 10 (2024) 369, https://doi.org/10.3390/jof10060369.
[26] R. Sharma, P. Toukola, J. Jordan, J. Vuorinen, N. Huynh, N. Durandin, M. Herrala, A. Primetta, J. Rysä, M. Österberg, P. Nousiainen, P. Laaksonen, R. Räisänen, Upcycling agricultural waste for functional interfaces: yellow onion skin-derived dyes for cellulosic materials, ACS Omega 10 (2025) 36511–36526, https://doi.org/10.1021/acsomega.5c05183.
[27] OECD, Test No. 442D: In Vitro Skin Sensitisation: ARE-Nrf2 Luciferase Test Method, OECD, 2022, https://doi.org/10.1787/9789264229822-en.
[28] S. Vesterlund, J. Paltta, A. Lauková, M. Karp, A.C. Ouwehand, Rapid screening method for the detection of antimicrobial substances, J. Microbiol. Methods 57 (2004) 23–31, https://doi.org/10.1016/j.mimet.2003.11.014.
[29] T. Jyske, J. Liimatainen, J. Tienaho, H. Brännström, D. Aoki, K. Kuroda, D. Reshamwala, S. Kunnas, E. Halmemies, E. Nakayama, P. Kilpeläinen, A. Ora, J. Kaseva, J. Hellström, V.S. Marjomäki, M. Karonen, K. Fukushima, Inspired by nature: fiber networks functionalized with tannic acid and condensed tannin-rich extracts of Norway spruce bark show antimicrobial efficacy, Front. Bioeng. Biotechnol. 11 (2023) 1171908, https://doi.org/10.3389/fbioe.2023.1171908.
[30] J. Tienaho, T. Sarjala, R. Franzén, M. Karp, Method with high-throughput screening potential for antioxidative substances using Escherichia coli biosensor katG'::lux, J. Microbiol. Methods 118 (2015) 78–80, https://doi.org/10.1016/j.mimet.2015.08.018.
[31] S. Kunnas, J. Tienaho, P. Kilpeläinen, M. Haapakoski, A. Perämäki, Q. Nie, Z. Lu, J. Huotari, S. Salo, M. Nurmi, M. Toivakka, C. Xu, A.E. Hagerman, V. Marjomäki, T. Jyske, Fabricating bio-based medical textiles with antimicrobial protection, Mater. Des. 265 (2026) 115895, https://doi.org/10.1016/j.matdes.2026.115895.
[32] Y. Yeo, Y. Shin, Inkjet printing of textiles using biodegradable natural dyes, Fibers Polym. 24 (2023) 1695–1705, https://doi.org/10.1007/s12221-023-00162-3.
[33] S. Vasile, M. Georgievska, C. Copot, A. De Raeve, Comparative analysis of elastic polyester sportswear fabrics with printed graphene patterns, Materials (Basel, Switzerland) 16 (2023) 2028, https://doi.org/10.3390/ma16052028.
[34] L. Ding, Y. Huang, X. Cai, S. Wang, Impact of pH, ionic strength and chitosan charge density on chitosan/casein complexation and phase behavior, Carbohydr. Polym. 208 (2019) 133–141, https://doi.org/10.1016/j.carbpol.2018.12.015.
[35] Q.Z. Wang, X.G. Chen, N. Liu, S.X. Wang, C.S. Liu, X.H. Meng, C.G. Liu, Protonation constants of chitosan with different molecular weight and degree of deacetylation, Carbohydr. Polym. 65 (2006) 194–201, https://doi.org/10.1016/j.carbpol.2006.01.001.
[36] Z. Ciesarová, M. Murkovic, K. Cejpek, F. Kreps, B. Tobolková, R. Koplík, E. Belajová, K. Kukurová, Ľ. Daško, Z. Panovská, D. Revenco, Z. Burčová, Why is sea buckthorn (Hippophae rhamnoides L.) so exceptional? A review, Food Res. Int. 133 (2020) 109170, https://doi.org/10.1016/j.foodres.2020.109170.
[37] E.J. Rupa, L. Kaliraj, S. Abid, D.-C. Yang, S.-K. Jung, Synthesis of a zinc oxide nanoflower photocatalyst from sea buckthorn fruit for degradation of industrial dyes in wastewater treatment, Nanomaterials (Basel, Switzerland) 9 (2019) 1692, https://doi.org/10.3390/nano9121692.

[38] M.G. Carneiro-da-Cunha, M.A. Cerqueira, B.W.S. Souza, J.A. Teixeira, A. A. Vicente, Influence of concentration, ionic strength and pH on zeta potential and mean hydrodynamic diameter of edible polysaccharide solutions envisaged for multinanolayered films production, Carbohydr. Polym. 85 (2011) 522–528, https://doi.org/10.1016/j.carbpol.2011.03.001.
[39] I. Szilagyi, G. Trefalt, A. Tiraferri, P. Maroni, M. Borkovec, Polyelectrolyte adsorption, interparticle forces, and colloidal aggregation, Soft Matter 10 (2014) 2479, https://doi.org/10.1039/c3sm52132j.
[40] A. Gupta, C.R. Ladino, T.H. Mekonnen, Cationic modification of cellulose as a sustainable and recyclable adsorbent for anionic dyes, Int. J. Biol. Macromol. 234 (2023) 123523, https://doi.org/10.1016/j.ijbiomac.2023.123523.
[41] C.E. Gherasim, M. Focşan, C. Ciont, A. Bunea, D. Rugină, A. Pintea, Stability and bioaccessibility of carotenoids from sea buckthorn pomace encapsulated in alginate hydrogel beads, Nutrients 16 (2024) 2726, https://doi.org/10.3390/nu16162726.
[42] K.S. Kontturi, T. Tammelin, L.-S. Johansson, P. Stenius, Adsorption of cationic starch on cellulose studied by QCM-D, Langmuir 24 (2008) 4743–4749, https://doi.org/10.1021/la703604j.
[43] S. Ali, M.A. Mughal, U. Shoukat, M.A. Baloch, S.H. Kim, Cationic starch (Q-TAC) pre-treatment of cotton fabric: influence on dyeing with reactive dye, Carbohydr. Polym. 117 (2015) 271–278, https://doi.org/10.1016/j.carbpol.2014.09.064.
[44] S. Zhang, W. Ma, B. Ju, N. Dang, M. Zhang, S. Wu, J. Yang, Continuous dyeing of cationised cotton with reactive dyes, Color. Technol. 121 (2005) 183–186, https://doi.org/10.1111/j.1478-4408.2005.tb00270.x.
[45] S. Ondaral, E. Çelik, O.Ç. Kurtuluş, E. Aşıkuzun, İ. Yakın, Chitosan adsorption on nanofibrillated cellulose with different aldehyde content and interaction with phosphate buffered saline, Carbohydr. Polym. 186 (2018) 192–199, https://doi.org/10.1016/j.carbpol.2017.12.028.
[46] M. Rinaudo, Chitin and chitosan: properties and applications, Prog. Polym. Sci. 31 (2006) 603–632, https://doi.org/10.1016/j.progpolymsci.2006.06.001.
[47] R. Fijan, M. Basile, R. Lapasin, S. Šostar-Turk, Rheological properties of printing pastes and their influence on quality-determining parameters in screen printing of cotton with reactive dyes using recycled polysaccharide thickeners, Carbohydr. Polym. 78 (2009) 25–35, https://doi.org/10.1016/j.carbpol.2009.03.022.
[48] O. Plohl, V. Kokol, A. Filipić, K. Fric, P. Kogovšek, Z.P. Fratnik, A. Vesel, M. Kurečič, J. Robič, L. Gradišnik, U. Maver, L.F. Zemljič, Screen-printing of chitosan and cationised cellulose nanofibril coatings for integration into functional face masks with potential antiviral activity, Int. J. Biol. Macromol. 236 (2023) 123951, https://doi.org/10.1016/j.ijbiomac.2023.123951.
[49] C.P. Hsu, R.H. Guo, C.C. Hua, C.-L. Shih, W.-T. Chen, T.-I. Chang, Effect of polymer binders in screen printing technique of silver pastes, J. Polym. Res. 20 (2013) 277, https://doi.org/10.1007/s10965-013-0277-3.
[50] H. Baniasadi, R. Ajdary, J. Trifol, O.J. Rojas, J. Seppälä, Direct ink writing of aloe vera/cellulose nanofibrils bio-hydrogels, Carbohydr. Polym. 266 (2021) 118114, https://doi.org/10.1016/j.carbpol.2021.118114.
[51] V. Kokol, Influence of hydroxyethyl and carboxymethyl celluloses on the rheology, water retention and surface tension of water-suspended microfibrillated cellulose, Cellulose 29 (2022) 7063–7081, https://doi.org/10.1007/s10570-022-04737-w.
[52] J. Wei, B. Wang, Z. Li, Z. Wu, M. Zhang, N. Sheng, Q. Liang, H. Wang, S. Chen, A 3D-printable TEMPO-oxidized bacterial cellulose/alginate hydrogel with enhanced stability via nanoclay incorporation, Carbohydr. Polym. 238 (2020) 116207, https://doi.org/10.1016/j.carbpol.2020.116207.
[53] M.O. Tuhin, N. Rahman, M.E. Haque, R.A. Khan, N.C. Dafader, R. Islam, M. Nurnabi, W. Tonny, Modification of mechanical and thermal property of chitosan–starch blend films, Radiat. Phys. Chem. 81 (2012) 1659–1668, https://doi.org/10.1016/j.radphyschem.2012.04.015.
[54] X. Liu, L. Yu, F. Xie, M. Li, L. Chen, X. Li, Kinetics and mechanism of thermal decomposition of cornstarches with different amylose/amylopectin ratios, Starch Stärke 62 (2010) 139–146, https://doi.org/10.1002/star.200900202.
[55] R.M.D. Soares, A.M.F. Lima, R.V.B. Oliveira, A.T.N. Pires, V. Soldi, Thermal degradation of biodegradable edible films based on xanthan and starches from different sources, Polym. Degrad. Stab. 90 (2005) 449–454, https://doi.org/10.1016/j.polymdegradstab.2005.04.007.
[56] J.J. Benitez, P. Florido-Moreno, J.M. Porras-Vázquez, G. Tedeschi, A. Athanassiou, J.A. Heredia-Guerrero, S. Guzman-Puyol, Transparent, plasticized cellulose-glycerol bioplastics for food packaging applications, Int. J. Biol. Macromol. 273 (2024) 132956, https://doi.org/10.1016/j.ijbiomac.2024.132956.
[57] E.A. Agustiany, D.S. Nawawi, W. Fatriasari, M.U. Wahit, H. Vahabi, D.S. Kayla, L. S. Hua, Mechanical, morphological, thermal, and fire-retardant properties of sustainable chitosan-lignin based bioplastics, Int. J. Biol. Macromol. 306 (2025) 141445, https://doi.org/10.1016/j.ijbiomac.2025.141445.
[58] L. Wu, S. Lv, D. Wei, S. Zhang, S. Zhang, Z. Li, L. Liu, T. He, Structure and properties of starch/chitosan food packaging film containing ultra-low dosage GO with barrier and antibacterial, Food Hydrocoll. 137 (2023) 108329, https://doi.org/10.1016/j.foodhyd.2022.108329.
[59] L. Valero, M. Gainche, C. Esparcieux, F. Delor-Jestin, H. Askanian, Vegetal polyphenol extracts as antioxidants for the stabilization of PLA: toward fully biobased polymer formulation, ACS Omega (2024) acsomega.3c07236, https://doi.org/10.1021/acsomega.3c07236.
[60] X. Lyu, X. Wang, Q. Wang, X. Ma, S. Chen, J. Xiao, Encapsulation of sea buckthorn (Hippophae rhamnoides L.) leaf extract via an electrohydrodynamic method, Food Chem. 365 (2021) 130481, https://doi.org/10.1016/j.foodchem.2021.130481.
[61] A.E. Torkamani, Z.A. Syahariza, M.H. Norziah, A.K.M. Wan, P. Juliano, Encapsulation of polyphenolic antioxidants obtained from *Momordica charantia* fruit within zein/gelatin shell core fibers via coaxial electrospinning, Food Biosci. 21 (2018) 60–71, https://doi.org/10.1016/j.fbio.2017.12.001.
[62] E. Nadim, P. Paraskar, E.J. Murphy, M. Hesabi, I. Major, Sustainable polyurethane coatings based on functional Camelina oil-based polyols, Ind. Crop. Prod. 204 (2023) 117274, https://doi.org/10.1016/j.indcrop.2023.117274.
[63] R.B. Doke, P.M. Paraskar, Y.N. Rajput, R.D. Kulkarni, Synthesis and characterization of green polyurethane coatings derived from Niger-seed-oil-based polyesteramide polyols, Euro. J. Lipid Sci. Tech. 124 (2022) 2100171, https://doi.org/10.1002/ejlt.202100171.
[64] A.B. Chaudhari, P.D. Tatiya, R.K. Hedaoo, R.D. Kulkarni, V.V. Gite, Polyurethane prepared from neem oil polyesteramides for self-healing anticorrosive coatings, Ind. Eng. Chem. Res. 52 (2013) 10189–10197, https://doi.org/10.1021/ie401237s.
[65] S. Chatterjee, S. Mahmood, A.R. Hilles, S. Thomas, S. Roy, V. Provaznik, E. L. Romero, K. Ghosal, Cationic starch: a functionalized polysaccharide based polymer for advancement of drug delivery and health care system - a review, Int. J. Biol. Macromol. 248 (2023) 125757, https://doi.org/10.1016/j.ijbiomac.2023.125757.
[66] L.C. Becker, W.F. Bergfeld, D.V. Belsito, R.A. Hill, C.D. Klaassen, D.C. Liebler, J. G. Marks, R.C. Shank, T.J. Slaga, P.W. Snyder, L.J. Gill, B. Heldreth, Safety assessment of glycerin as used in cosmetics, Int. J. Toxicol. 38 (2019) 6S–22S, https://doi.org/10.1177/1091581819883820.
[67] P. Baldrick, The safety of chitosan as a pharmaceutical excipient, Regul. Toxicol. Pharmacol. 56 (2010) 290–299, https://doi.org/10.1016/j.yrtph.2009.09.015.
[68] S. Babaeipour, P. Nousiainen, E. Kimiaei, J. Tienaho, N. Kohlhuber, R. Korpinen, K. Kaipanen, M. Österberg, Thin multifunctional coatings for textiles based on the layer-by-layer application of polyaromatic hybrid nanoparticles, Mater. Adv. 5 (2024) 6114–6131, https://doi.org/10.1039/D4MA00085D.
[69] S. Kunnas, J. Tienaho, T. Holmbom, S. Sutela, J. Liimatainen, K. Kaipanen, R. Jääskeläinen, S. Sääski, R.I. Korpinen, Antimicrobial treatments with chitosan microencapsulated angelica (*Angelica archangelica*) and marsh Labrador tea (*Rhododendron tomentosum*) supercritical CO_2 extracts in linen-cotton jacquard woven textiles, Text. Res. J. 94 (2024) 2253–2272, https://doi.org/10.1177/00405175241247024.
[70] E.K. Gebeyehu, R. Shresth, T. Saha, J. Tienaho, U. Jauhiainen, A.A. Tarhini, A. R. Tehrani-Bagha, Antibacterial and physicomechanical properties of cellulosic nonwovens functionalized with chitosan: a study on interaction effects of influencing factors and assessment methods, Bioresour. Bioprocess. 12 (2025) 11, https://doi.org/10.1186/s40643-025-00843-2.
[71] D. Massella, S. Giraud, J. Guan, A. Ferri, F. Salaün, Textiles for health: a review of textile fabrics treated with chitosan microcapsules, Environ. Chem. Lett. 17 (2019) 1787–1800, https://doi.org/10.1007/s10311-019-00913-w.
[72] J. Nath, M. Dewan, A. Ghosh, S.S. Ray, J.T. Orasugh, B. Lahiri, D. Chattopadhyay, A. Adhikari, Chitosan-based adsorbents for remediation of toxic dyes from wastewater: a review on adsorption mechanism, reusability, machine learning based modeling and future perspectives, Int. J. Biol. Macromol. 311 (2025) 143388, https://doi.org/10.1016/j.ijbiomac.2025.143388.
[73] M. Vakili, M. Rafatullah, B. Salamatinia, A.Z. Abdullah, M.H. Ibrahim, K.B. Tan, Z. Gholami, P. Amouzgar, Application of chitosan and its derivatives as adsorbents for dye removal from water and wastewater: a review, Carbohydr. Polym. 113 (2014) 115–130, https://doi.org/10.1016/j.carbpol.2014.07.007.
[74] AATCC Test Method 61–2009: Colorfastness to Laundering, Accelerated, 2009.
[75] B. Yang, H. Kallio, Composition and physiological effects of sea buckthorn (Hippophaë) lipids, Trends Food Sci. Technol. 13 (2002) 160–167, https://doi.org/10.1016/S0924-2244(02)00136-X.
[76] D.B. Rodriguez-Amaya, Food Carotenoids: Chemistry, Biology, and Technology, 1st ed., Wiley, 2015 https://doi.org/10.1002/9781118864364.
[77] D. Cristea, G. Vilarem, Improving light fastness of natural dyes on cotton yarn, Dyes Pigments 70 (2006) 238–245, https://doi.org/10.1016/j.dyepig.2005.03.006.
[78] P.D.D.F. Santos, F.T.V. Rubio, M.P. Da Silva, L.S. Pinho, C.S. Favaro-Trindade, Microencapsulation of carotenoid-rich materials: a review, Food Res. Int. 147 (2021) 110571, https://doi.org/10.1016/j.foodres.2021.110571.
[79] J.N. Chakraborty, J.N. Chakraborty, Assessment of fastness of dyeings, 2014, https://doi.org/10.1201/b18243-37.
[80] J.Y. Hu, L. Hes, Y. Li, K.W. Yeung, B.G. Yao, Fabric touch tester: integrated evaluation of thermal–mechanical sensory properties of polymeric materials, Polym. Test. 25 (2006) 1081–1090, https://doi.org/10.1016/j.polymertesting.2006.07.008.
[81] J.F. Mendes, R.T. Paschoalin, V.B. Carmona, A.R. Sena Neto, A.C.P. Marques, J. M. Marconcini, L.H.C. Mattoso, E.S. Medeiros, J.E. Oliveira, Biodegradable polymer blends based on corn starch and thermoplastic chitosan processed by extrusion, Carbohydr. Polym. 137 (2016) 452–458, https://doi.org/10.1016/j.carbpol.2015.10.093.
[82] R. Shi, Q. Liu, T. Ding, Y. Han, L. Zhang, D. Chen, W. Tian, Ageing of soft thermoplastic starch with high glycerol content, J. Appl. Polym. Sci. 103 (2007) 574–586, https://doi.org/10.1002/app.25193.
[83] E.D.M. Teixeira, C. Lotti, A.C. Corrêa, K.B.R. Teodoro, J.M. Marconcini, L.H. C. Mattoso, Thermoplastic corn starch reinforced with cotton cellulose nanofibers, J. Appl. Polym. Sci. 120 (2011) 2428–2433, https://doi.org/10.1002/app.33447.
[84] P.-Y. Mikus, S. Alix, J. Soulestin, M.F. Lacrampe, P. Krawczak, X. Coqueret, P. Dole, Deformation mechanisms of plasticized starch materials, Carbohydr. Polym. 114 (2014) 450–457, https://doi.org/10.1016/j.carbpol.2014.06.087.